Impact of sensing and infusion site dependent dynamics on insulin bolus based meal compensation

Konstanze Kölle [*,**] **Anders Fougner** [*,**] **Øyvind Stavdahl** [*]

* Department of Engineering Cybernetics, Norwegian University of Science and Technology, Trondheim, Norway (e-mail: {konstanze.koelle, anders.fougner, oyvind.stavdahl}@ntnu.no).
** Central Norway Regional Health Authority (RHA), Trondheim, Norway

Abstract: Meals are most challenging in the regulation of blood glucose levels (BGL) in diabetes mellitus type 1, whether it is automated, semi-automated or manually controlled. The common subcutaneous (SC) route for glucose sensing and insulin administration suffers from large latencies. This paper investigates the impact of glucose sensing and insulin absorption dynamics on the achievable glucose regulation when insulin boluses are triggered by a meal detection system.
In silico patients from the academic version of the UVa/Padova simulator are studied. The sub-models of glucose sensing and insulin absorption are adjusted to allow simulations with different time delays and time constants. Meals are detected with published methods based on threshold-checking of continuous glucose monitoring data.
Slow glucose sensing dynamics delay the meal detection. Delayed meal detection can be compensated to some extent by exact knowledge about the insulin absorption. The combination of slow glucose sensing and slow insulin administration reduces the effect of insulin boluses on the postprandial BGL. The classical SC approach is, therefore, at high risk of large BGL excursions despite meal detection.

Keywords: Artificial pancreas or organs; Biomedical system modeling, simulation and visualization; Control of physiological and clinical variables

1. INTRODUCTION

The hormone insulin enables the body to utilize energy contained in food and keep homeostasis of the blood glucose level (BGL). The lack of natural insulin secretion in diabetes mellitus type 1 (DM1) necessitates exogenous insulin administration. Sensor-augmented insulin pumps combine insulin infusion with continuous glucose monitoring (CGM). According to a pre-programmed protocol, insulin is continuously administered into the subcutaneous (SC) tissue while the SC glucose concentration is monitored.

People using insulin pumps have to initiate insulin boluses to avoid heavily elevated BGL after meals. The postprandial BGL excursions depend not only on the amount of consumed carbohydrates (CHO) but also on the glucose absorption from the intestines. This variation is illustrated in Fig. 1. Aside from the glucose rate of appearance in blood, also the onset of insulin action and its duration must be considered when estimating the size of prandial insulin boluses. It is, for example, recommended to administer the boluses ahead of the meal to compensate for the insulin absorption dynamics from the SC tissue (Cobry et al., 2010). But even several hours after the meal, slowly absorbed insulin can cause hypoglycemia. With that in mind, it is hardly surprising that many people are struggling to estimate the bolus size (Burdick et al., 2004; Brazeau et al., 2013). Furthermore, occasionally omitted insulin boluses compromise the outcome of the therapy.

A fully automated system, an artificial pancreas (AP), is the goal of worldwide research efforts. Most clinical studies on AP have focused on closed-loop solutions including feed-forward prandial insulin boluses. The AP clinical trial database provided by the Doyle Group (http://thedoylegroup.org/apdatabase/) lists 61 published clinical trials from 2004–2015 that used meal announcements, whereas only 23 trials refrained from meal announcements in the same period. Two studies from 2016 demonstrate the potential benefit of meal detection. Pinsker et al. (2016) compared the performance of the two controller types model predictive control (MPC) and proportional integral derivative (PID) in 20 adult subjects. The study protocol included an unannounced lunch with 65 g COH. Neither MPC nor PID were able to maintain the BGL in the target range after the unannounced meals for all studied subjects. On average, less than 50% of the 5 first postprandial hours were spent in the target range (70–180 mg/dL). In another clinical study, eight adult subjects underwent closed-loop control with a beta-cell-imitating algorithm (similar to a conventional PID controller) for 24 hours (Reddy et al., 2016). An unannounced dinner with 80 g CHO and a partly announced lunch were consumed
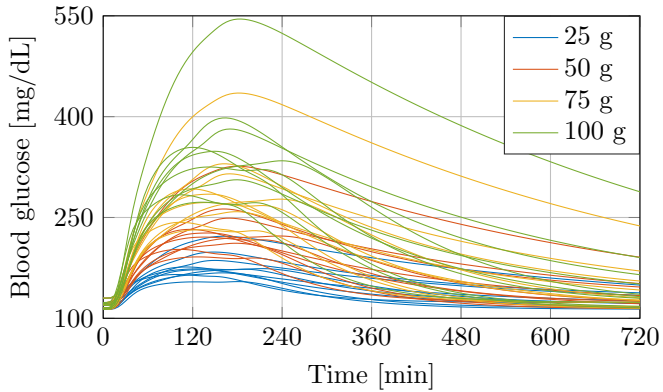
Fig. 1. Glucose concentration following meals with different carbohydrate content for 10 simulated adults. High variability between subjects is demonstrated.
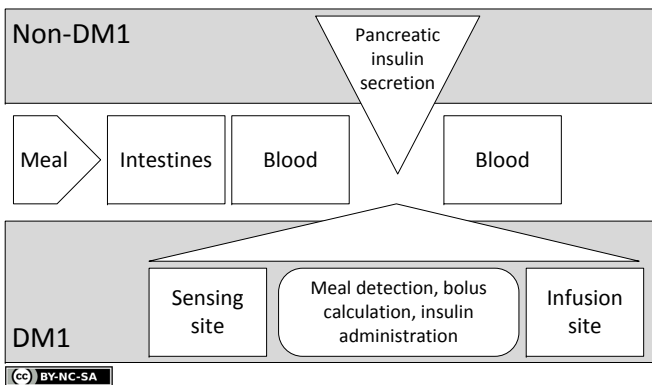

Fig. 2. Meal compensation in people with diabetes mellitus type 1 (DM1) and with normal physiology (Non-DM1). This figure is licensed under a Creative Commons BY-NC-SA 4.0 license.

during the study. The lunch contained 50 g CHO, of which 25 g were announced to the controller. The glucose concentration, measured with a SC sensor, stayed in the target range (70–180 mg/dL) for less than 50% of the time.

Meals can be explicitly detected to trigger meal boluses or to adjust the controller tuning. Suggested methods for meal detection based on threshold checking use the raw CGM data either directly or revised by removing measurement noise using a linear noise model in a Kalman filter (KF) (Dassau et al., 2008; Lee and Bequette, 2009; Harvey et al., 2014).

In the study of Harvey et al. (2014), the mean time of detection of meals with 25, 50, 75 and 100 g CHO was at least 30 min using the common 5-min sampling rate of CGM devices. Although the postprandial peaks and the time spent in hyperglycemia could be significantly reduced by their meal detection method, the studied *in silico* subjects still remained in hyperglycemia for 1.5 hours after a meal with 75 g COH (Harvey et al., 2014). In the course of a year that easily adds up to more than 1500 hours with insufficiently controlled BGL.

The primary reasons for the poor performance of meal detection algorithms are most likely the slow dynamics of glucose and insulin diffusion between the SC tissue and blood (Stavdahl et al., 2016). Figure 2 illustrates

the course of meal compensation. During meal digestion, the glucose is absorbed from the intestines causing the BGL to rise. The speed and peak of glucose appearance in blood depends on meal composition and size, previously consumed meals, and probably other factors. In people without DM1, the pancreas reacts to increased BGL by directly secreting insulin into the blood. A person with DM1 lacks this immediate, natural feedback. Instead, the blood transports the glucose first through the whole body where it diffuses into tissues that are used as measuring sites. Based on the glucose measurements, the artificial meal response begins: The meal is detected, an appropriate bolus size estimated and the bolus administered. The insulin is absorbed from the infusion site into the blood and distributed through the body, eventually lowering the glucose concentration. The glucose appearance from blood to the measuring site and the insulin absorption from the infusion site into the blood are part of the physiology of the body. Despite faster-absorbed insulin analogues (Heise et al., 2015), the physiology presents a number of profound limitations.

An artificial pancreas must not put the user on an unnecessary risk of hypoglycemia. Therefore, significantly increased insulin infusion rates, be it by more aggressive controller actions or superimposed insulin boluses, are only defensible if a meal has occurred. To detect a meal with a certain probability takes time. This study investigates the impact of glucose sensing dynamics on the time to meal detection and the achievable glucose normalizing effect of insulin boluses administered upon meal detection. The aim is to answer the question whether or not meals can be sufficiently compensated with an insulin bolus whose effect is delayed by meal detection and the insulin absorption dynamics. If a "perfect" insulin bolus upon detection cannot compensate a meal in an "ideal" setting, an artificial pancreas without meal announcements will not achieve good glucose regulation in real-world scenarios.

2. METHODS

2.1 Simulator

The academic version of the UVA/Padova T1DM simulator S2013 (Dalla Man et al., 2014) is used for simulations. In this study, only adult subjects are simulated. Among the simulator options, no-error models are selected for the insulin pump and the sensor. The simulator model describes the glucose insulin metabolism in people with DM1. The sub-models for glucose sensing and insulin absorption are adjusted to study the impact of different dynamics.

2.2 Sub-model of glucose sensing

The sub-model for glucose sensing is:

$$\frac{\mathrm{d}G_{sens}}{\mathrm{d}t} = \frac{1}{\tau_G}\left(G_p(t - \theta_G) - G_{sens}(t)\right), \qquad (1)$$

where G_{sens} (mg/dL) is the sensed glucose concentration at the measurement site, G_p (mg/dL) is the plasma glucose concentration, τ_G (min) is the time constant related to the measurement site, and θ_G (min) is the time delay from plasma to the measurement site. The dynamics of
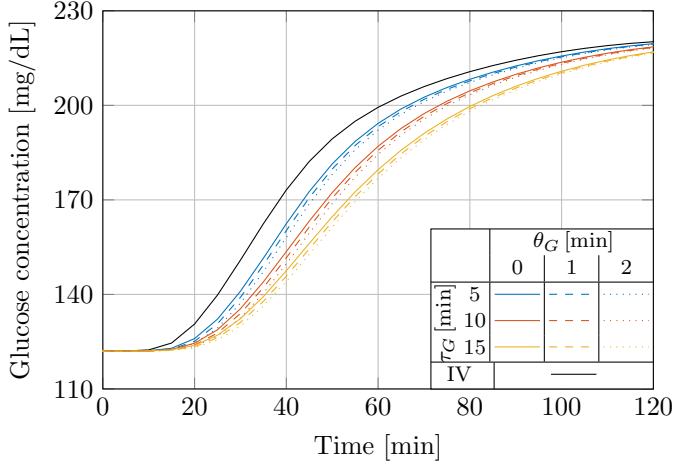
Fig. 3. Sensed glucose concentration with different sensing dynamics within the first two hours following a meal with 50 g carbohydrate content without prandial insulin bolus for one adult subject.

physiological glucose diffusion and the sensor dynamics are combined in the glucose sensing dynamics.

The subject-specific time constant of SC glucose sensing in the adult population of the simulator ranges from 7 to 11 min. Reported mean values for SC glucose appearance including the sensor dynamics in pigs are $\tau_G = 13$ min and $\theta_G = 2$ min (Burnett et al., 2014), while faster dynamics of $\tau_G = 6$ min and $\theta_G = 1$ min have been observed for peritoneal glucose sensing in pigs (Burnett et al., 2014; Fougner et al., 2016). However, the SC route excluding sensor dynamics can be as fast as $\tau_G = 5$ min and $\theta_G = 1$ min for single subjects under well controlled clinical conditions (Basu et al., 2015). Influencing factors are the time since sensor insertion, the perfusion and fat content of the SC tissue. Based on the earlier mentioned studies, the parameters of (1) are varied as follows:

- Time constant $\tau_G \in \{5, 10, 15\}$ min,
- Time delay $\theta_G \in \{0, 1, 2\}$ min.

Figure 3 illustrates the sensed glucose concentration for the chosen glucose sensing dynamics following a meal with 50 g of carbohydrates.

2.3 Sub-model of insulin absorption

The insulin absorption is modeled as a two-compartment model where only insulin from the second compartment reaches the plasma (Lee et al., 2013), although the dynamics of some routes may be better described by more complex models. In contrast to Lee et al. (2013), the latency is differentiated into a time constant and a time delay. The following model replaces the insulin absorption dynamics (Eqs. (A15),(A16) from Dalla Man et al. (2014)):

$$R_{ai}(t) = \frac{1}{\tau_I} I_2(t - \theta_I), \qquad (2)$$

$$\frac{dI_1}{dt} = -\frac{1}{\tau_I} I_1(t) + IIR(t), \qquad (3)$$

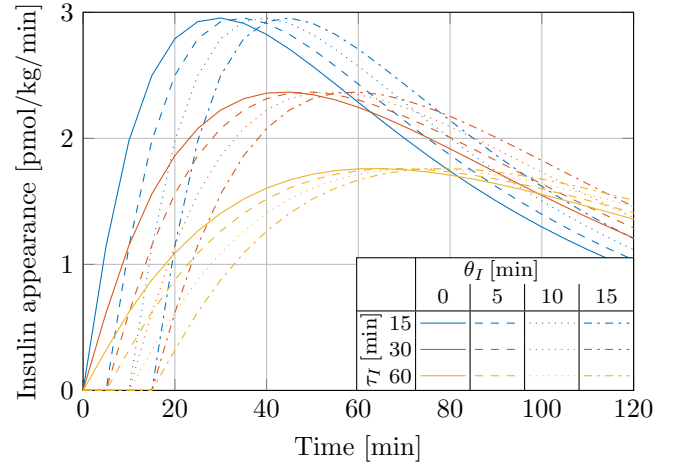$$\frac{dI_2}{dt} = \frac{1}{\tau_I} I_1(t) - \frac{1}{\tau_I} I_2(t), \qquad (4)$$

Fig. 4. Rate of insulin appearance in blood with different insulin absorption dynamics for one adult subject following an insulin bolus of 4 IU at t = 0.

where R_{ai} (pmol/kg/min) is the rate of appearance of insulin in the blood from the infusion site, I_1 and I_2 (pmol/kg) are the amount of insulin in compartment 1 and 2 of the infusion site, IIR (pmol/kg/min) is the insulin infusion rate, τ_I (min) and θ_I (min) are the time constant and the time delay of the insulin absorption from the infusion site to plasma. This two-compartment structure was achieved by setting the original model parameters in (A15),(A16) (Dalla Man et al., 2014) to $k_{a1} = 0\,\text{min}^{-1}$, $k_{a2} = 1/\tau_I\,\text{min}^{-1}$ and $k_d = 1/\tau_I\,\text{min}^{-1}$.

Pharmacokinetic studies state times between 1 and 12 min for the onset of insulin appearance in plasma dependent on the insulin type (Heise et al., 2015) and the route of administration (Micossi et al., 1986; Oskarsson et al., 2000). The onset of appearance in plasma is represented by the time delay θ_I in (2). Lee et al. (2013) identified time constants for the two-compartment model without time delay for different insulin analogues administered subcutaneously. The time constants are lower when the time delay is considered. The insulin administration parameters in (2) to (4) are varied as follows:

- Time constant $\tau_I \in \{15, 30, 60\}$ min,
- Time delay $\theta_I \in \{0, 5, 10, 15\}$ min.

Figure 4 shows that insulin appears in plasma later and at a lower rate for slower dynamics.

2.4 Meal detection method

The applied methods for meal detection use the information contained in pure CGM data. More advanced methods relying on any kind of model or statistical information are not considered here in order to reduce the effect of model mismatch and other uncertainties. By this restriction, thresholds on the measured glucose (G_sens), its rate of change (G'_sens) and its acceleration (G''_sens) remain as tuning parameters.

The postprandial glucose excursions vary significantly for different carbohydrate contents and subjects, as illustrated in Fig. 1. For the ten adult subjects, the maximum blood glucose elevation ranges from 40 mg/dL for a 25 g-CHO

meal in adult 10 to 430 mg/dL for a 100 g-CHO meal in adult 7. This wide range indicates the challenge of choosing suitable thresholds.

The detection logic of the *Glucose Rate Increase Detector* (GRID) from Harvey et al. (2014) was applied in this study. A meal is detected according to GRID at instant k if:

$$G(j) > G_{\min} \qquad \text{for } j = k \qquad (5)$$

and

$$G'(j) > G'_{\min,3} \qquad \text{for } j = k-2, k-1, k \qquad (6)$$
$$\text{or} \quad G'(j) > G'_{\min,2} \qquad \text{for } j = k-1, k. \qquad (7)$$

The rate of change $G'(j)$ in (6),(7) is derived using the three-point Lagrange interpolating polynomial. The CGM data is passed through a preprocessing section that removes spikes and noise by guaranteeing a maximum rate of change of 3 mg/dL/min and a low-pass filter before the detection logic is applied. Best detection results were achieved in the study of Harvey et al. (2014) with the tuning parameters $G_{\min} = 130$ mg/dL, $G'_{\min,3} = 1.5$ mg/dL/min, and $G'_{\min,2} = 1.6$ mg/dL/min for both clinical and simulated data sets.

This study applies also the meal detection methods from Dassau et al. (2008) and Lee and Bequette (2009). Similar to the GRID algorithm, these methods detect meals when CGM data and its first and second derivatives exceed defined thresholds. More details can be found in the original publications.

The detection thresholds that are reported in the original publications are used. Thereby, the same tuning is applied for all subjects. As the glucose response to meals is highly diverse between subjects, individual tuning may improve the detection capabilities but is tested only for the GRID algorithm. The following individualized thresholds are defined in this study:

(1) $G_{\min} = 1.05\, G_b$,
(2) $G'_{\min,3} = 1.5\, \frac{\Delta G_{\max}(50\,\text{g})}{\Delta t_{\max}(50\,\text{g})}$,
(3) $G'_{\min,2} = 1.6\, \frac{\Delta G_{\max}(50\,\text{g})}{\Delta t_{\max}(50\,\text{g})}$.

The fraction $\Delta G_{\max}(50\,\text{g})/\Delta t_{\max}(50\,\text{g})$ describes the maximum glucose deviation from the basal level after the ingestion of 50 g CHO divided by the time it takes to reach this maximum from the start of ingestion. These values could be gained by an oral glucose tolerance test with regular sampling of blood glucose.

The thresholds of the original studies were not tuned for the same group of patients, i.e. adults (Lee and Bequette, 2009; Harvey et al., 2014) vs. children (Dassau et al., 2008), which may influence the detection performance. Consequently, absolute numerical results are not indicative of the fundamental performance of each algorithm. Rather, it is the relative sensitivity of each algorithm to different dynamics that is the focus of this study.

The cited detection methods have been published for CGM data sampled every 5 min. A more frequent sampling of 1 min shall be used in this study to investigate the differences between the varied dynamics. In order to apply the published threshold values nevertheless, the detection

Table 1. Simulated open-loop scenarios with different timing of prandial insulin bolus administration.

Scenario	Time of bolus	Meal detection
Uncompensated meal	-	no
Announced meal	at meal start	no
Detected meal	at detection	yes

intervals of 5 min are kept but simultaneous runs of the same detection algorithm are started one minute apart from each other. The detection statistics of whichever run detects the meal first are taken. Common CGM devices sample every 3 or 5 min but 1-minute sampling may become standard with increasing accuracy of CGM devices. However, the results of this study cannot be directly compared with results from other studies with different sampling rates.

2.5 Prandial insulin boluses

In order to compare the best achievable glucose regulation in each scenario, the following two criteria are used to determine the bolus size (Visentin et al., 2016):

(C1) $G(t = 120\,\text{min}) < 8.9$ mmol/L
(C2) $G(t > 0) > 3.9$ mmol/L

The bolus size is increased by 0.1 international units of insulin (IU) if criterion C1 is violated, as long as criterion C2 is fulfilled.

It is not always possible to keep the BGL between 3.9 and 8.9 mmol/L. Nevertheless, criterion C2 safeguards against hypoglycemic events that present an asymmetrically higher risk than hyperglycemic episodes. This analysis does thus not weigh hypo- and hyperglycemia against each other but rather focuses on the comparison of hyperglycemic excursions.

2.6 Scenarios

Single meal scenarios are simulated. All meals last for 15 min. The subjects are controlled at their basal glucose concentration before the meals start. This is achieved by administering insulin continuously at the subject-specific basal rate defined in the simulator. Prandial insulin boluses are superimposed.

No faults, neither pump nor sensor related such as occlusion or pressure induced sensor attenuation, are simulated. The sensor signal contains no outliers.

The three main scenarios are listed in table 1. The scenario of an uncompensated meal describes the situation without prandial insulin bolus. The resulting glucose regulation of this scenario serves as example of manual glucose therapy where the insulin bolus is forgotten. An announced meal starts at the same time as the insulin bolus is injected. This is common practice in closed-loop set-ups using announced meals and allows to study how the insulin absorption dynamics influence the postprandial glucose response. The additional impact of the glucose sensing dynamics is investigated in the detected meal scenario where the insulin bolus is administered when the meal is detected. The bolus calculation and insulin administration happens in all scenarios immediately without delay.
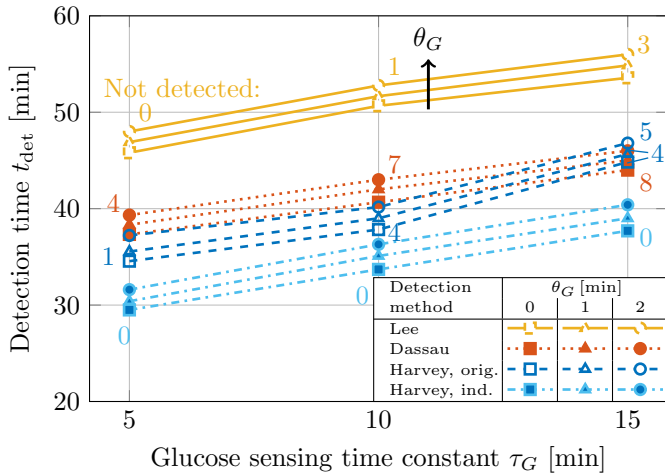
Fig. 5. Average detection time of 50 g meal for 10 subjects dependent on time constant τ_G for different time delays θ_G. Numbers indicate number of non-detected meals. Harvey's method with original (orig.) and individualized (ind.) thresholds.

Table 2. Percentage of non-detected meals from in total 120 50 g meals (12 for each of 10 subjects) for CGM data without noise and with noise (PACF = 0.25 as simulator option).

| Detection method | Noise-free | | Noise | |
| | Glucose dynamics | | Glucose dynamics | |
	Fast	Slow	Fast	Slow
Lee	0%	30%	7%	23%
Dassau	40%	80%	38%	71%
Harvey original	10%	50%	20%	57%
Harvey individual	0%	0%	0%	0%

2.7 Metrics

The performance of meal detection is described by the time of detection after meal start (t_{det}). The percentage of time that is spent within the target range of 3.9–10 mmol/L (70–180 mg/dL) and the tight target range of 4.4–7.8 mmol/L (80–140 mg/dL) are often used as metrics for the performance of glucose regulation. By design, the prandial insulin boluses will always lead to a minimum BGL slightly above 3.9 mmol/L (70 mg/dL). The minimum BGL and time in tight target are thus not suitable for comparison. The maximum glucose concentration (G_{max}) and the mean glucose concentration (G_{mean}) can, however, be used as measures for the performance of glucose regulation.

Some methods do not detect all meals for all subjects. Non-detected meals are considered in the statistics by G_{max}, G_{mean}, t_{target} for uncompensated meals. For t_{det}, the number of undetected meals is indicated in the figure.

3. RESULTS

3.1 Glucose sensing dynamics

The first step in meal mitigation is meal detection. Detection times are compared for different glucose sensing dynamics in Fig. 5. The upwards-trend shows that the

time of detection increases with slower glucose dynamics. Moreover, the number of non-detected meals (indicated by the numbers next to the marks) is increasing with increasing time constant τ_G, whereas the number is the same for different time delays θ_G. The only exception is one subject where an increase of the sensing delay to two minutes renders the meal undetectable to the original method by Harvey. All meals are detected by Harvey's method with individualized thresholds. As a result of the earlier detection, the glucose deviations at detection are lower (not shown), and the insulin bolus can be administered earlier.

The percentage of non-detected meals for noise-free and noisy CGM data is compared in table 2. Fast glucose dynamics result in the detection of more meals for all methods. The methods by Lee and Bequette (2009) and Dassau et al. (2008) reveal slightly more meals if noise is present. This, together with a higher number of false meal detections (not shown), demonstrates that the tuning of thresholds is important and should possibly be individualized.

3.2 Insulin absorption dynamics

Table 3 summarizes the glycemic measures for the uncompensated and the announced meal scenarios for a meal with 50 g CHO. A missed meal bolus results in elevated glucose levels for prolonged time, and the percentage of time that is spent in the target range is therefore as low as 27.9% for the 50 g meal. When the meal is announced, this percentage can be increased to 100% with fast insulin absorption dynamics, whereas the glucose concentration exceeds the target range for almost all subjects with the slowest insulin absorption dynamics ($\tau_I = 60$ min, $\theta_I = 15$ min).

Slower dynamics result in delayed insulin appearance in plasma. The maximum and mean glucose concentrations, G_{max} and G_{mean}, are thus increasing. Another effect of the delayed insulin appearance is that less insulin can be used to lower the BGL. If the amount of insulin that was found for the fastest dynamics were administered using the slowest route, the glucose concentration would fall below the lower limit of 3.9 mmol/L causing hypoglycemia.

3.3 Combined dynamics

Administering the prandial insulin bolus upon meal detection, the time that is spent in target range is significantly increased compared to the 28% after an uncompensated meal (Table 3). Figure 6 further reveals, unsurprisingly, that faster dynamics of glucose sensing and insulin absorption prolong the time in target independent of the detection method and its particular tuning. When the method by Harvey et al. (2014) is used with individualized thresholds, the 50 g meal is detected for all subjects leading to a significant increase of time spent in target range for the slow glucose dynamics. The percentage converges to the announced meal scenario as the dynamics become faster. The average time in target is significantly lower using the other detection methods because the non-detected meals remain uncompensated.

Table 3. Comparison of the effect of bolus time on glucose regulation. Meal compensation characteristics for a meal with 50 g of carbohydrates during the 6 hours after meal onset. Average values of all ten subjects are given for each measure with standard deviations in parentheses.

Scenario	Uncompensated	Announced		
Insulin absorption dynamics		fast $\tau_I = 15\,\text{min}, \theta_I = 0\,\text{min}$	medium $\tau_I = 30\,\text{min}, \theta_I = 10\,\text{min}$	slow $\tau_I = 60\,\text{min}, \theta_I = 15\,\text{min}$
Insulin bolus [IU]	-	6.3 (2.5)	5.7 (2.1)	5.1 (1.8)
$G_{\max}$ [mg/dL]	234.6 (36.4)	144.1 (5.4)	167.8 (7.5)	183.6 (11.6)
G_{mean} [mg/dL]	201.9 (29.3)	95.7 (3.6)	103.9 (4.6)	117.7 (6.5)
t_{target} (3.9–10 mmol/L) [%]	27.9 (14.5)	100 (0)	100 (0)	92.9 (6.6)

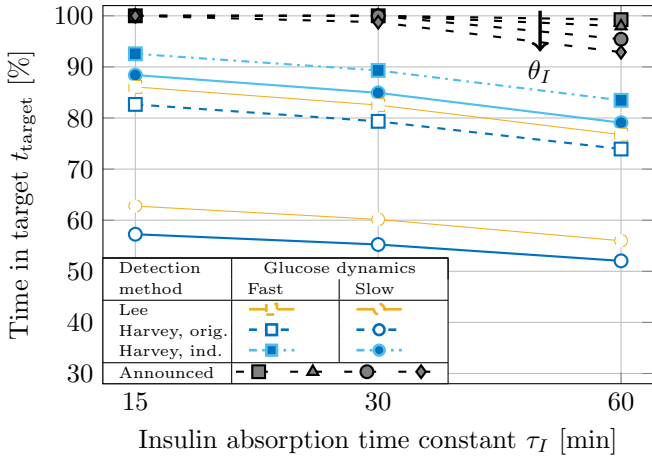Fig. 6. Average time in target (3.9–10 mmol/L) within the 6 hours after a 50 g meal for 10 subjects comparing different time constants τ_I. Values are averaged for time delays $\theta_I \in \{0, 5, 10, 15\}$ min if not indicated otherwise.
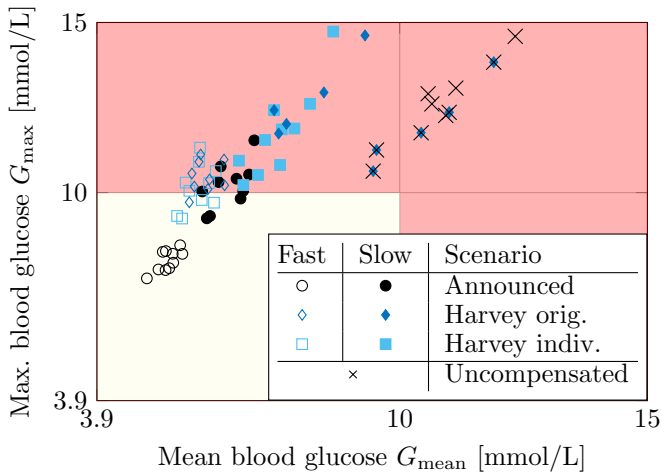

Fig. 7. Average maximum and mean glucose concentrations during the 6 hours following a 50 g meal for 10 subjects for the fastest dynamics (open marks) and slowest dynamics (filled marks).

Figure 7 illustrates the inter-individual variation. Each mark represents the maximum and mean glucose concentration for one subject during the 6 hours following a 50 g meal. After an announced meal, all subjects remain within the target range when the insulin absorption is fast (black open circles). This good glucose regulation is almost approached using Harvey's method with origi-

nal and individualized thresholds and the fastest glucose sensing dynamics (dark-blue open diamonds, light blue open squares). However, several subjects exceed the upper bound of 10 mmol/L. Larger glucose excursions follow with slow glucose sensing and insulin absorption dynamics (filled marks), and the inter-subject variation becomes larger. For some subject, the meal is not even detected, resulting in an uncompensated meal.

4. DISCUSSION

This study demonstrates that the glucose sensing dynamics and insulin absorption dynamics have similar impact on the performance of glucose regulation achieved by threshold-based meal detection, using the glucose levels and its rates-of-change, and subsequent insulin bolus administration. Slow glucose sensing dynamics delay the detection of the meal and thus the insulin administration but most critical with respect to meal mitigation is whether the meal is detected at all. A delayed detection of medium-sized meals can be well compensated by administering an optimal insulin bolus upon detection. However, the ability to keep the glucose concentration within the target range decreases with larger meal sizes (not shown). Estimating prandial boluses is a large challenge in real-world scenarios because the insulin sensitivity and the characteristics of insulin absorption must be considered and are highly variable. Moreover, the timing of the insulin bolus affects the maximum amount of insulin that can be used without causing hypoglycemia.

The time until meal detection based on threshold-checking of CGM data could be reduced by measuring glucose concentration in other tissues than the SC tissue. The IP route is currently being investigated (Burnett et al., 2014; Fougner et al., 2016). A quick onset of the glucose-lowering effect of administered insulin significantly contributes to the performance of meal compensation. Insulin formulations with faster absorption kinetics from the SC tissue are being developed (Heise et al., 2015). Alternatively, the peritoneal cavity could be chosen as a site for insulin infusion (Micossi et al., 1986; Oskarsson et al., 2000; Renard et al., 2010) to enhance the meal mitigation. Faster dynamics may even obviate the need for explicit meal detection. Nevertheless, binary information about meals could increase the safety by allowing more aggressive control actions until the meal disturbance is rejected, whereas the aggressiveness of the controller is otherwise low in order to be robust to noise. A detected meal could also directly trigger the administration of insulin boluses.

Neither faults or noise nor changing physiological dynamics that appear in real systems are considered in this study.

That decision was made on purpose to focus on the impact of the overall dynamics. The influence of the tuning as a tradeoff between high specificity and sensitivity is reduced by that. The first step of a sufficient meal compensation is an accurate meal detection. Mathematically more advanced methods for meal detection should be investigated in order to face the intra-subject variability in real-world scenarios. The detection could also benefit from additional information beyond CGM data. Anticipatory approaches, for example, take into account meal prior probabilities based on general or individual eating behavior and sleeping times in order to improve the meal detection (Patek et al., 2009; Cameron et al., 2012). The impact of glucose sensing dynamics on the estimation of meal sizes, and thus allowable bolus sizes, should be analyzed in subsequent work. Both closed-loop scenarios and meals with overlapping BGL responses should be investigated in this context.

5. CONCLUSION

Glucose sensing and insulin absorption dynamics have similar impact on the achievable glucose regulation with insulin bolus administration upon detection of medium-sized meals. Delayed detection can be compensated if the insulin absorption is well known but the regulation is significantly deteriorated if both dynamics are slow. A system with subcutaneous glucose sensing and insulin infusion might therefore be insufficient. However, most important is that the meal is detected at all. Using detection algorithms based on threshold checking on CGM data and its derivatives, the thresholds should be individualized because of the high inter-subject variability and the higher number of false positive detections.

REFERENCES

Basu, A., Dube, S., Veettil, S., et al. (2015). Time lag of glucose from intravascular to interstitial compartment in type 1 diabetes. *J Diabetes Sci Technol*, 9(1), 63–68.

Brazeau, A.S., Mircescu, H., Desjardins, K., et al. (2013). Carbohydrate counting accuracy and blood glucose variability in adults with type 1 diabetes. *Diabetes Res Clin Pract*, 99(1), 19–23.

Burdick, J., Chase, H.P., Slover, R.H., et al. (2004). Missed insulin meal boluses and elevated hemoglobin [a.sub.1c] levels in children receiving insulin pump therapy. *Pediatrics*, 113(3), 613.

Burnett, D.R., Huyett, L.M., Zisser, H.C., Doyle, III, F.J., and Mensh, B.D. (2014). Glucose sensing in the peritoneal space offers faster kinetics than sensing in the subcutaneous space. *Diabetes*, 63(7), 2498–2505.

Cameron, F., Niemeyer, G., and Bequette, B.W. (2012). Extended multiple model prediction with application to blood glucose regulation. *J Process Control*, 22(8), 1422–1432.

Cobry, E., McFann, K., Messer, L., et al. (2010). Timing of meal insulin boluses to achieve optimal postprandial glycemic control in patients with type 1 diabetes. *Diabetes Technol Ther*, 12(3), 173–7.

Dalla Man, C., Micheletto, F., Lv, D., et al. (2014). The UVA/Padova type 1 diabetes simulator: New features. *J Diabetes Sci Technol*, 8(1), 26–34.

Dassau, E., Bequette, B.W., Buckingham, B.A., and Doyle, III, F.J. (2008). Detection of a meal using continuous glucose monitoring implications for an artificial β-cell. *Diabetes care*, 31(2), 295–300.

Fougner, A.L., Kölle, K., Skjærvold, N.K., et al. (2016). Intraperitoneal glucose sensing is sometimes surprisingly rapid. *Modeling, Identification and Control*, 37(2), 121–131.

Harvey, R.A., Dassau, E., Zisser, H., Seborg, D.E., and Doyle, F.J. (2014). Design of the glucose rate increase detector a meal detection module for the health monitoring system. *J Diabetes Sci Technol*, 307–320.

Heise, T., Zijlstra, E., Rikte, T., et al. (2015). Faster-acting insulin aspart using continuous subcutaneous insulin infusion (CSII): Earlier onset of exposure and greater early pharmacokinetic (PK) and pharmacodynamic (PD) effects than insulin aspart. *Diabetes*, 64, A256–A256.

Lee, H. and Bequette, B.W. (2009). A closed-loop artificial pancreas based on model predictive control: Human-friendly identification and automatic meal disturbance rejection. *Biomed Signal Process Control*, 4(4), 347–354.

Lee, J.J., Dassau, E., Zisser, H., et al. (2013). The impact of insulin pharmacokinetics and pharmacodynamics on the closed-loop artificial pancreas. In *2013 IEEE 52nd Annual Conference on Decision and Control (CDC)*, 127–132.

Micossi, P., Cristallo, M., Librenti, M.C., et al. (1986). Free-insulin profiles after intraperitoneal, intramuscular, and subcutaneous insulin administration. *Diabetes Care*, 9(6), 575–578.

Oskarsson, P.R., Lins, P.E., Backman, L., and Adamson, U.C. (2000). Continuous intraperitoneal insulin infusion partly restores the glucagon response to hypoglycaemia in type 1 diabetic patients. *Diabetes & metabolism*, 26(2), 118.

Patek, S.D., Bequette, B.W., Breton, M., et al. (2009). In silico preclinical trials: Methodology and engineering guide to closed-loop control in type 1 diabetes mellitus. *J Diabetes Sci Technol*, 3(2), 269–282.

Pinsker, J.E., Lee, J.B., Dassau, E., et al. (2016). Randomized crossover comparison of personalized MPC and PID control algorithms for the artificial pancreas. *Diabetes Care*, 39(7), 1135–1142.

Reddy, M., Herrero, P., Sharkawy, M.E., et al. (2016). Metabolic control with the bio-inspired artificial pancreas in adults with type 1 diabetes: A 24-hour randomized controlled crossover study. *J Diabetes Sci Technol*, 10(2), 405–13.

Renard, E., Place, J., Cantwell, M., Chevassus, H., and Palerm, C.C. (2010). Closed-loop insulin delivery using a subcutaneous glucose sensor and intraperitoneal insulin delivery feasibility study testing a new model for the artificial pancreas. *Diabetes Care*, 33(1), 121–127.

Stavdahl, Ø., Fougner, A.L., Kölle, K., et al. (2016). The artificial pancreas: A dynamic challenge. *IFAC-PapersOnLine*, 49(7), 765–772.

Visentin, R., Giegerich, C., Jäger, R., et al. (2016). Improving efficacy of inhaled technosphere insulin (afrezza) by postmeal dosing: In-silico clinical trial with the university of virginia/padova type 1 diabetes simulator. *Diabetes Technol Ther*, 18(9), 574–585.